Seismic data processing using the pyramid transform

Barry Hung
Veritas DGC
Singapore
barry_hung@veritasdgc.com

Carl Notfors
Veritas DGC
Crawley, U.K.
carl_notfors@veritasdgc.com

Shuki Ronen
Veritas DGC
Houston, U.S.
shuki_ronen@veritasdgc.com

SUMMARY

The pyramid transform is a resampling of data in the *f-x-y* domain (Fourier transform over time but not over space) that gives rise to frequency dependent spatial grids with a relationship that the sampling interval is inversely proportional to the frequency. Such transformation is reversible for wave-fields and it gives rise to an important feature that *f-x-y* prediction filters in the pyramid domain are frequency independent. This leads to the fact that, in the pyramid domain, the prediction filters can be estimated from a range of frequencies that have higher signal-to-noise ratio. The resulting filters are therefore more reliable and they can then be applied across the whole frequency range to perform prediction filtering.

Using the prediction filtering in the pyramid domain, we demonstrate how it can be used in seismic data processing for trace interpolation, data regularisation and filling in missing traces. We show that, with synthetic and field data examples, prediction filters estimated in the pyramid domain are more robust against noise, aliased events and conflicting dips than the ones estimated in the conventional *f-x-y* domain.

Key words: Pyramid transform, prediction filtering.

INTRODUCTION

Seismic data are often spatially undersampled in 3-D exploration. Trace interpolation, a well-known solution to this sampling deficiency, is often used to estimate unrecorded traces from a spatially undersampled dataset. Various interpolation methods for handling aliased events have been proposed over the years and some of their features, such as computational efficiency and data accuracy, have been compared (Abma et al., 2003). One of the methods that was used as a benchmark in the comparison studies is called the *f-x* domain prediction filtering method, which is used routinely in data processing. This technique is based on the principle that linear events are predictable in the *f-x* domain without any prior knowledge of the dips of the events (Spitz, 1991). It operates on 2-D regular data in the temporal frequency (*f*) domain in such a way that, for an interpolation order of λ, a spatial prediction filter is designed at *f* with trace spacing δx and then applied to predict data at frequency λf with trace spacing $\delta x/\lambda$.

Apart from sparsely sampled, seismic data are also typically irregularly sampled along spatial coordinates. Hence, it is necessary to regularise the acquired data because advanced processing techniques such as wave-equation migration and multiple attenuation require the input data to be regularly sampled. Therefore, there is a need to extend the *f-x* method to work on irregularly sampled data and this has been addressed by Crawley (1999). However, prediction filtering in the conventional *f-x* domain has been shown that it has the difficulty of handling complicated structures (Hung *et al*, 2004a). We demonstrated that prediction filters estimated in the pyramid domain are more robust against noise and conflicting dips than ones estimated in the conventional *f-x* domain. This is because wave-fields can be reconstructed with fewer samples at low temporal frequencies without violating sampling theory (Sun and Ronen, 1996). This then gives rises to the useful feature that a single prediction filter can be estimated in the pyramid domain from a range of frequencies, hence the estimation can normally be performed with a higher signal-to-noise (S/N) ratio, and the resulting filter is more reliable.

In the following, we first explain what the pyramid transform is and how it can be used for trace interpolation using prediction filtering on regularly sampled data. We then extend the transform to data regularisation and reconstruction of missing traces by using frequency-independent prediction error filter as a constraint to an inverse problem. Finally, we illustrate the advantages of the pyramid method through synthetic and filed data examples.

THEORY – PYRAMID TRANSFORM

To perform the pyramid transform, a 3-D dataset is first Fourier transformed in time. This transforms the data to the *f-x-y* domain. Within this domain, the data is then spatially resampled in such a way that the resulting spatial interval is inversely proportional to the frequency. That is, the lower the frequency, the smaller the number of data samples. This leads to a pyramid shaped sampling (hence the name for the transform). Moreover, the low frequencies are not over-parameterized after the transform which makes frequency dependent grids more suitable for either inversion or interpolation. The pyramid transform is based on Shannon's sampling theorem, so it is invertible. In other words, if one performs the forward and then the inverse pyramid transform, one can recover the original input data.

Mathematically, the way to spatially resample an input data in the pyramid domain is guided by the well-known equation that relates the maximum non-aliased frequency f_m to a dip angle θ with trace interval δx:

$$f_{\mathbf{m}} = \frac{v}{4\delta x \sin\theta} \qquad (1)$$

where v is medium velocity. Rearranging equation (1) and setting $\theta=90^o$ give rise to the following equation:

$$\sin\theta = \frac{\boldsymbol{v}}{4\boldsymbol{f}'\delta\boldsymbol{x}} = 1 \qquad (2)$$

where f' is the critical frequency. Equation (2) indicates that for frequencies below f', one may resample the spatial intervals in such a way that the new intervals Δx_f (a function of f) fulfill the relationship of $\Delta x_f = v/4f$ and yet retain dip information up to 90°; whereas, for frequencies above f', one can only obtain dip information of $\theta_{max} = \sin^{-1}(v/4f'\delta x)$ with the original trace interval δx. The use of the critical frequency f' for the pyramid transform is schematically illustrated in figure 1 where figure 1a shows the input data cube in the *f-x-y* domain and figure 1b the data volume after the pyramid transform. One may observe that the volume of the data has shrunk significantly after the pyramid transform. Hence, the pyramid is equivalent to the cube in the conventional *f-x-y* domain in terms of information amount but with smaller data volume. In addition, the base of the pyramid occurs at frequency f'; above f' the data arrangement is same as the corresponding section in the *f-x-y* domain.

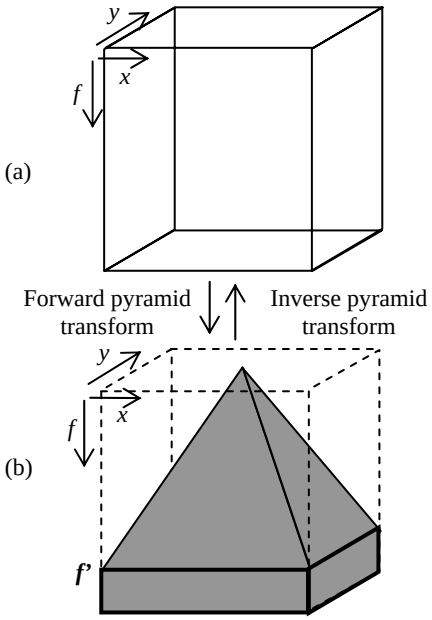

Figure 1. (a) Input data cube in the original *f-x-y* domain. (b) Data volume after the pyramid transform.

The feature of frequency dependent grids in the pyramid domain has an important application for spatial prediction filtering. That is, the prediction filter is independent of temporal frequency and hence a single prediction filter can be estimated from a range of frequencies below the critical frequency. This makes the estimation of the filter not only efficient, because the process needs not be repeated for each frequency, but also more stable and robust against noise, since a frequency range with high S/N ratio can always be chosen for the estimation (Hung *et al*, 2004b).

So far, the discussion has been limited to regularly sampled data, i.e. δx is a constant. When the input data is not regularly sampled or has missing traces, prediction filtering in the pyramid domain can still be used for data reconstruction. In this case, prediction error filters (PEFs) are used as numerical regularisation operators to constrain the forward modeling operator that maps the model space to the data space with the context of an inversion. This can be expressed in matrix notation as:

$$\mathbf{D} \approx \mathbf{L}\,\mathbf{m} \qquad (3)$$

$$\mathbf{0} \approx \mathbf{D}\,\mathbf{m} \qquad (4)$$

where **d** is the data vector, **L** is the forward-modeling operator, **m** is the model vector and **D** is the numerical regularisation operator. Equations (3) and (4) are also known as the data-fitting and model-shaping goals, respectively, and give rise to a least-squares solution that can be obtained iteratively using the conjugate-gradient method (Claerbout, 1992).

The effect of using PEF as **D** in Equation (4) to constrain the inversion is to assume that the model **m** is linear and therefore predictable. The assumption of linearity is often fulfilled by processing the data with small window; whereas, the predictability of the model allows the PEF estimated at low temporal frequencies to act as a regularisation operator that constrains the inversion at higher frequencies in the pyramid domain. Since the spatial bandwidth is small for low temporal frequencies, this leads to better stability together with an improved ability to regularise the data and, or, to reconstruct the signal in gaps. This is preferable to estimating the PEF at each individual frequency, as in the conventional *f-x* domain.

APPLICATIONS

(i) Trace interpolation for regularly sampled data

Figure 2a shows a linear event that is contaminated with noise (5–70 Hz) but has the highest S/N ratio in the frequency range of 10-15 Hz. The even-numbered traces of this input were decimated. After the decimation, the event is aliased above 50 Hz. The decimated traces were then reproduced by the conventional *f-x* method and the result is depicted in figure 2b. The difference between the original input and the *f-x* interpolation result is displayed in figure 2c. One may observe from the difference plot that the conventional *f-x* method does not perform well for this example even for one linear event. It is because it uses frequencies with low S/N ratio to obtain the prediction filter for interpolation, i.e., for instance, the aliased frequency of 60 Hz uses the prediction filter estimated at 30 Hz, which has low S/N ratio, for interpolation. On the contrary, when only the frequency range with the highest S/N ratio (in this case 10-15 Hz) is used for the estimation of the prediction filter in the pyramid domain, a greatly improved interpolation result, as shown in figure 2d, is obtained. From the difference plot shown in figure 2e, it is apparent that the pyramid method performs better than the conventional *f-x* method in the presence of noise.

In cases where conflicting dips as well as noise pose a problem to the conventional *f-x* method, the pyramid method may be used for generating better results. Figure 3a shows the migrated image of subline 242 of the SEG/EAGE model. Its highest S/N ratio is in the frequency range of 10-20 Hz for most parts of the area. Again, the even-numbered traces were removed and then reproduced by interpolation. Figure 3b displays the result obtained by the conventional *f-x* method. Using the frequency range of 10-20 Hz for the estimation of the prediction filter, the interpolation result obtained by the pyramid method is plotted in figure 3c. It can be seen that the pyramid method reproduces the data much better than the conventional *f-x* method. In particular, the area on top of the salt dome and the area around the salt in the timegate of 1.5-2.2 s, where conflicting dips of the events make it difficult for

the conventional *f-x* method to estimate the prediction filters accurately. Moreover, the computational time needed to generate figures 3b and 3c was almost the same because, in the pyramid method, the extra time needed to transform the data to the pyramid domain is offset by the time that is saved in estimating only one prediction filter for a frequency range.

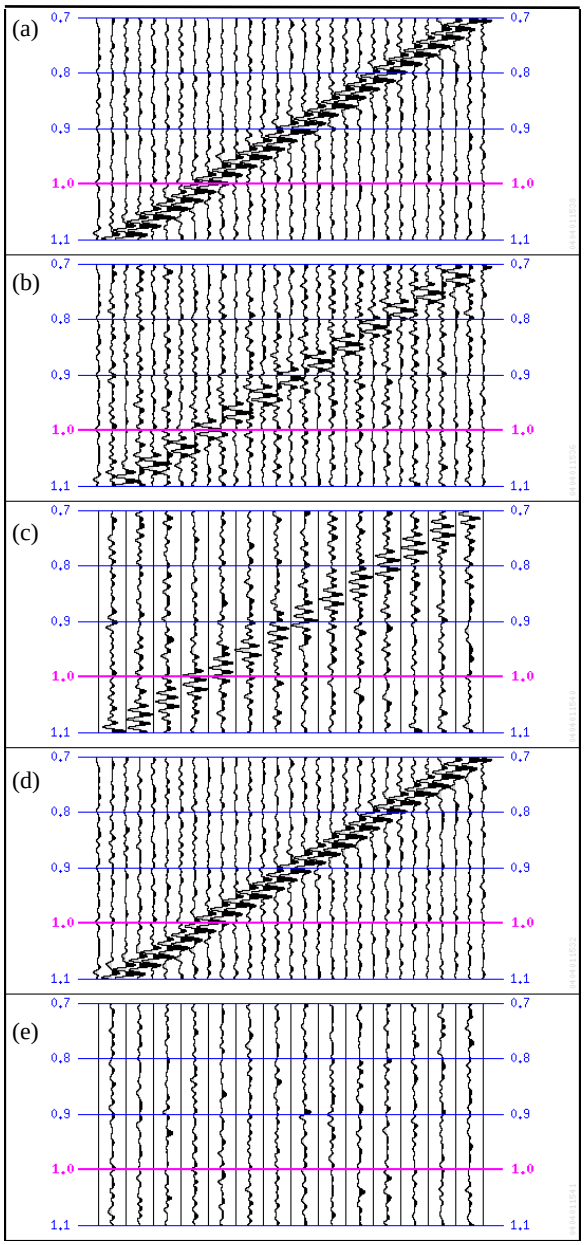

Figure 2. (a) Original input before its even-numbered traces are removed. (b) Interpolation result using the conventional f-x method. (c) The difference plot between (a) and (b). (d) Interpolation result using the pyramid method. (e) The difference plot between (a) and (d).

(ii) Data reconstruction for irregularly sampled data with missing traces

Figure 4a shows a synthetic dataset with four dipping events that are irregularly sampled, but with 34 traces missing out of the original 100 traces. The two steepest events are aliased and the maximum gap is equivalent to three traces. This represents quite a challenging test. The *f-k* spectrum of the data is shown in Figure 4d. The reconstruction result using the pyramid method is displayed in Figure 4b, and its *f-k* spectrum depicted in Figure 4e. This latter plot clearly shows that the algorithm handles the aliased events well. The difference between the original and reconstructed data set is given in Figure 4c, and confirms that the amplitude of the signal has successfully been recovered.

Finally, we test our method on a real data set. Figure 5a shows a common-offset section from a 3-D survey after binning. In this case, many of the traces are not located at the bin centers, and the data contain missing traces, and crossing events, as well as amplitude changes along the events themselves. Figure 5b displays the reconstruction result obtained with the pyramid transform method. It can be seen that the holes have been filled, the amplitudes are well recovered and the continuity of the events enhanced.

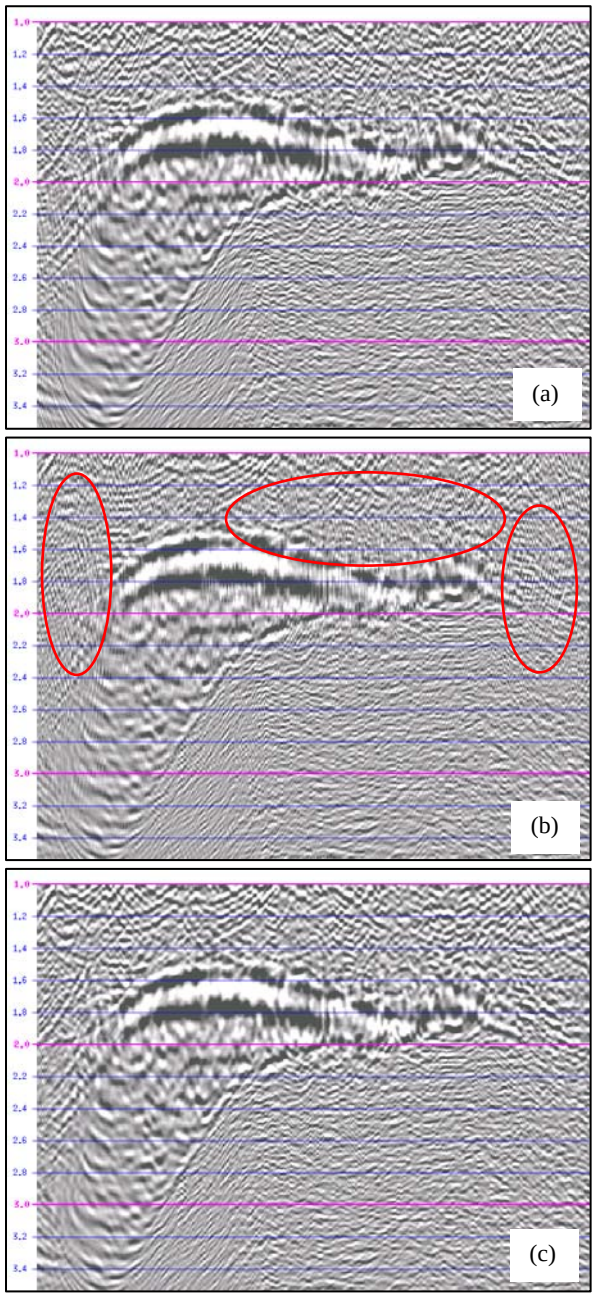

Figure 3. (a) Original migrated subline of the SEG/EAGE model before its even-numbered traces are removed. (b)

Interpolation result using the conventional *f-x* method. (c) Interpolation result using the pyramid method.

CONCLUSIONS

We have discussed the application of the pyramid transform for trace interpolation and data regularisation. By using the property that the prediction filter is independent of frequency in the pyramid domain, we have shown that the prediction (error) filter estimated from a range of low frequencies can be used to predict data at higher frequencies for regularly sampled data and constrain the inverse problem for higher frequencies for irregularly sampled data. We have also shown that the proposed method works well with synthetic and real data.

REFERENCES

Abma, R., and Kabir, N., 2003, Comparisons of interpolation methods in the presence of aliased events: 73rd Meeting, SEG, Expanded Abstracts, 1909-1912.

Claerbout J. F., 1992, Earth soundings analysis: Processing versus inversion: Black-well Scientific Publications.

Crawley, S., 1999, Interpolating missing data: convergence and accuracy, *t* and *f*: Stanford Exploration Project Report (SEP-102), 1-14.

Hung B., Notfors C. and Ronen S., 2004a. Robust prediction filtering using the pyramid transform: 66th Mtg.: Eur. Assn. Geosci. Eng., Expanded Abstracts, D-30.

Hung B., Notfors C. and Ronen S., 2004b. Seismic trace interpolation using the pyramid transform: 74th Meeting, SEG, Expanded Abstracts, 2017-2020.

Spitz S., 1991, Seismic trace interpolation in the F-X domain: Geophysics, **56**, no. 12, 2727-2741.

Sun Y. and Ronen S., 1996. The pyramid transform and its application to signal/noise separation: Stanford Exploration Project Report (SEP-93), 161-176.

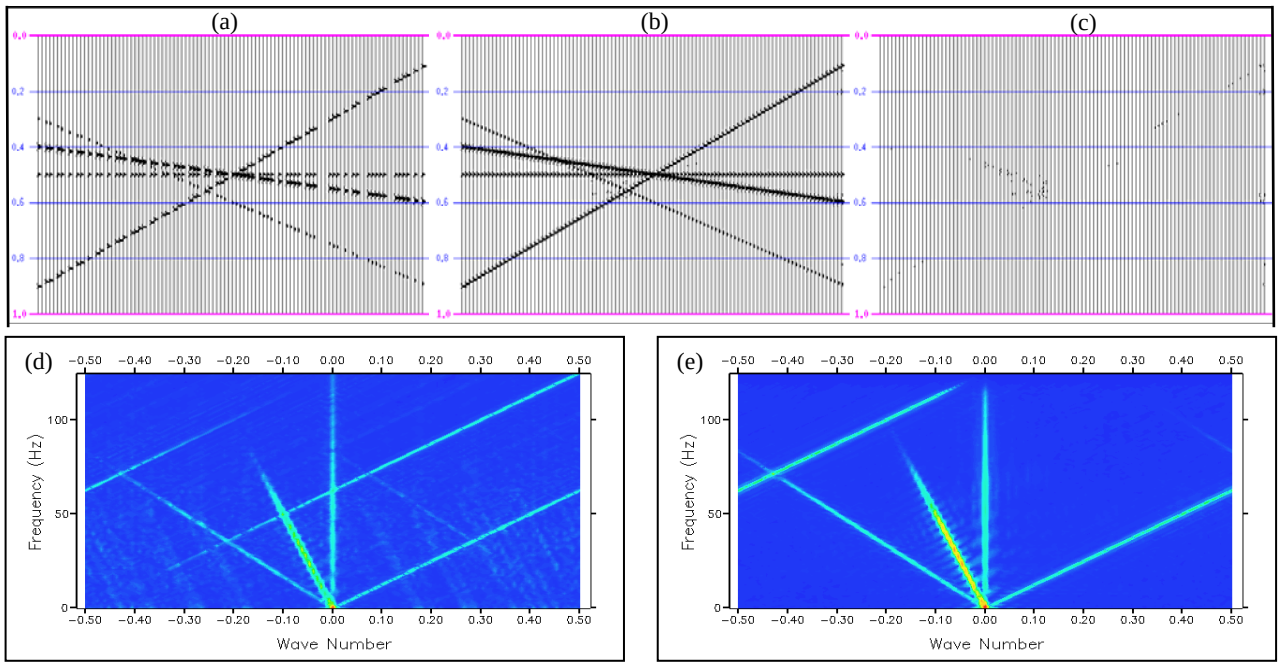

Figure 4. Synthetic data example with 34 traces missing in an irregularly sampled data of a total of 100 traces. (a) Input data. (b) Reconstructed result. (c) Difference between original data and reconstructed result. (d) *f-k* spectrum of the input. (e) *f-k* spectrum of the reconstructed result.

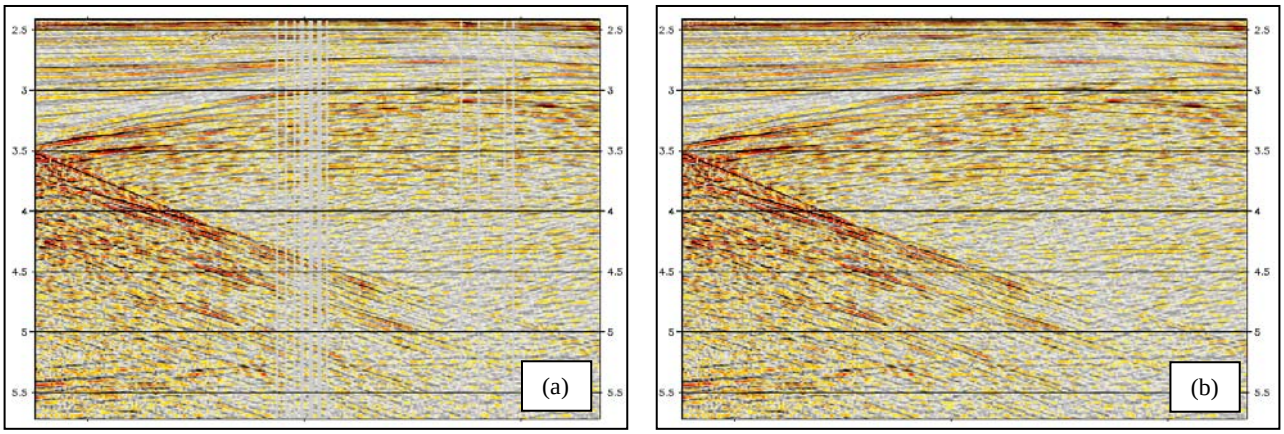

Figure 5. Real data application. (a) Input irregularly-sampled data with missing traces. (b) Output regularly sampled data.